

# Localized Laser Transmission Bonding for Microsystem Fabrication and Packaging

S.Theppakuttai, D.B. Shao, and S.C. Chen, Dept. of Mechanical Engineering,  
The University of Texas at Austin, Austin, Texas, USA. *E-mail:* scchen@mail.utexas.edu

## Abstract

This paper reports a method using localized laser heating to bond silicon and glass wafers directly. A pulsed Nd:YAG laser (1064 nm, 12 ns) is transmitted through the glass wafer and absorbed by the silicon wafer. Bonding is realized when the glass wafer is in immediate contact with the silicon wafer. A continuous wave He-Ne laser (633 nm, 20 mW) is used for probing the transient melting and resolidification of the silicon surface upon pulsed laser heating. This transmission bonding process is conducted locally while the entire wafer is maintained at a low temperature, which is especially useful in fabricating or packaging temperature-sensitive materials or devices. The bonded areas are studied in detail using a scanning electron microscope (SEM) and a chemical analysis is done to understand the bonding mechanism. Numerical simulation is also carried out using the finite element method to predict the local temperature change of both the glass wafer and the silicon wafer during laser heating.

**Keywords:** Laser Bonding, Pulsed Laser Heating, Silicon Wafers, Glass Wafers

## Nomenclature

$c$  = specific heat (J/kgK)  
 $h$  = specific enthalpy (J/m<sup>3</sup>)  
 $I$  = intensity (W/m<sup>2</sup>)  
 $J$  = pulse energy (J)  
 $k^0$  = thermal conductivity (W/mK)  
 $Q_{ab}$  = heat generation (J/m<sup>3</sup>)  
 $R$  = reflectivity  
 $r$  = cylindrical coordinate  
 $T$  = temperature (K)  
 $t$  = time (s)  
 $z$  = coordinate along propagation (m)  
 $\alpha$  = absorption coefficient (1/m)  
 $\rho$  = density (kg/m<sup>3</sup>)

## Subscript

$g$  = glass  
 $p$  = pulse  
 $Si$  = silicon

## Introduction

Bonding is a widely used method in microelectromechanical systems (MEMS) fabrication and packaging. The excellent mechanical strength of silicon combined with the electrical insulation, chemical durability, and optical transparency of glass makes the silicon-glass couple the most employed material combination in MEMS. Another reason for this combination is the very small difference in the coefficient of thermal expansion between glass and silicon (Rogers and Kowal 1995). Anodic bonding and fusion bonding are the most common techniques used for silicon-glass and silicon-silicon wafer joining, respectively. The anodic bonding method utilizes a high electric field (about 1000 V), and fusion bonding is done in a furnace at temperatures as high as 1100°C. Therefore, both techniques tend to damage the prefabricated microelectronics or pre-seeded biomolecules and thus exclude the use of thermally sensitive materials for micro and meso devices. Moreover, both anodic and fusion bonding are conducted along the entire wafer and so they do not provide an effective solution to integrating discrete micro or nano structures onto a chip to realize lab-on-a-chip or other integrated microsystems. Furthermore, in cases where hermetic sealing is desired, the residual gases trapped in the hermetic cavity can induce plastic deformation in thin silicon membranes as the gases expand due to the high temperature associated with the bonding process (Henmi et al. 1994).

To overcome the abovementioned drawbacks, researchers have been trying to find reliable bonding processes that can be conducted under a low temperature. Unfortunately, these new processes are highly dependent on the bonding materials, surface treatment, and surface flatness (Bower and Chin 1997; Bower, Ismail, and Roberts 1993). An alter-

native approach to bonding based on the concept of localized heating has been introduced in recent years. Lasers, with their selectivity, precision, and low heat distortion, are an attractive choice for providing localized heating. Laser transmission joining is a fast and single-step process with “direct-write” capability. This approach makes it possible to bond microstructures and pre-immobilized biomolecules for sensing, actuation, and even computing in BioMEMS. A pulsed 355 nm laser was used for glass-to-silicon bonding in the presence of indium as an intermediate layer. To achieve selective bonding, a masking material was also used (Luo and Lin 2002). Both pulsed and continuous wave (CW) 1064 nm lasers have been employed for the bonding process in the presence of aluminum or gold as an intermediate bonding layer (Mescheder et al. 2002; Wild, Gillner, and Poprawe 2001). However, in most cases, the presence of an intermediate bonding layer is undesirable as it increases the size of the device and complicates the fabrication of many devices. Also, little work has been done to investigate the physical mechanism of the laser-assisted bonding process for micro and meso systems.

In this paper, a 1064 nm pulsed nanosecond laser is employed for the bonding process in the absence of an intermediate layer. The bonding area is probed for obtaining more information about the melting process. A low-powered CW He-Ne laser is used for in situ monitoring to provide information about the melting time based on the change in the reflectivity of silicon (Xu, Grigoropoulos, and Russo 1996; Hatano et al. 2000). To understand the localized bonding process, it is essential to have a theoretical or numerical model that could calculate the temperature distribution. In this work, the temperature profiles during laser bonding are calculated using the finite element method.

## Experimental Setup

The samples used for bonding were silicon (Nova Electronic Materials, Texas) and Pyrex™ glass (Bullen Ultrasonics, Ohio) wafers of thickness 500 μm. The surface roughness of the silicon and glass samples to be joined is in the nanometer scale (< 2 nm), as the wafers were well polished. Before loading the samples, care is taken to ensure that the samples are clean and free of any contaminants. For

this reason, they are first cleaned in ethanol solution followed by rinsing in deionized water. The samples are then dried with nitrogen gas. The clean samples are then loaded in between two aluminum plates with an opening in the center, and pressure is applied continuously until the end of the bonding process by bolting the plates together. The tight contact of both the joining partners caused by the pressing device ensures elimination of small air gaps as well as good heat conduction to the glass. When locally heated by the laser radiation, the glass is softened due to heat conduction from the silicon surface and, after cooling, the adhesion of the joint compounds results in a tight joining.

The schematic of the experimental setup is shown in *Figure 1*. A 1064 nm pulsed Nd:YAG laser of 12 ns pulsewidth is used for the bonding process. The output of the laser beam passes through an aperture and a beam splitter, which is used to split the incident laser beam into two—one part to be used for bonding and the other for measuring the energy of pulses used for bonding. The sample is mounted on a 3-D stage and the laser beam is focused to a spot size of 800 μm diameter by using a plano-convex lens (diameter = 2.54 cm and focal length = 5.08 cm). By adjusting the working distance between the lens and the sample, the bonding area can be varied. The bonding process depends on the melting area as well as melting duration of silicon and the subsequent heat conduction to glass. Therefore, to ensure proper bonding, an in situ monitoring of the melting

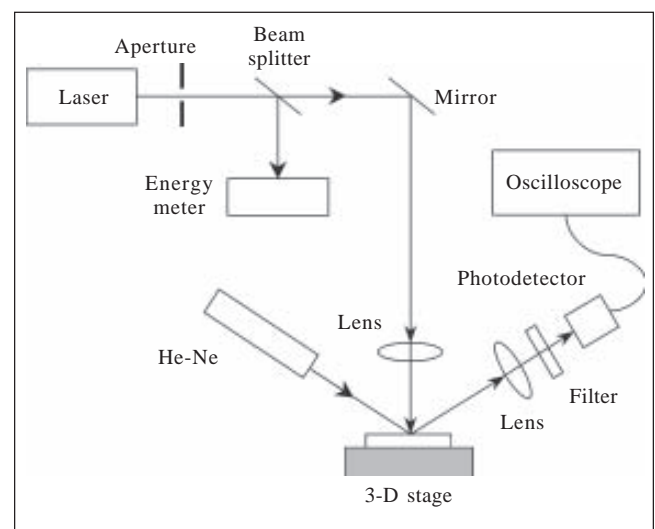


Figure 1  
Schematic of Experimental Setup

process is very important. A low-powered CW He-Ne laser (633 nm, 20 mW) is used as a probing beam for online monitoring. To make sure the measurement of melting time is accurate, the detection beam is focused onto the heating area. This is achieved by expanding the He-Ne beam using a beam expander and focusing it using a plano-convex lens with a shorter focal length (diameter = 2.54 cm and focal length = 2.54 cm). The incident probing beam reflected by the silicon sample is collected by a fast silicon PIN photodiode with 1 ns rise/fall time. The photodiode is connected to a digitizing oscilloscope with 500 MHz bandwidth and 1 GSa/s sampling rate operated at single-shot acquisition mode (1 ns time resolution). To eliminate the emission signal and other reflected wavelengths from the heated silicon surface, optical filters were used, which only transmit the probing laser wavelength. The heating pulse is used as a trigger to capture the reflected detecting beam. On heating, the reflectivity of silicon changes, and this results in a change in the intensity of the signal captured by the oscilloscope, which provides melting duration information during bonding.

## Numerical Simulation

The laser heating process is a highly nonlinear phenomenon due to the Gaussian distribution of laser energy in time and space. In addition, material properties like thermal conductivity and optical properties such as absorption coefficient are strong nonlinear functions of temperature. As a result, an analytical solution of the heat transfer and melting problem is less practical and numerical results were sought instead.

The heat conduction process during and after laser irradiation has been studied before (Chen and Tien 1994; Abraham and Halley 1987; Bloisi and Vicari 1988). Previous researchers have shown that the Fourier heat conduction equation is still valid for nanosecond laser processing in micrometer regimes (Burgener and Reedy 1982). In line with this, the Fourier heat conduction equation is used in this work to find the temperature distribution. In earlier works, one-dimensional heat conduction models were employed (Chen and Tien 1994; Abraham and Halley 1987; Bloisi and Vicari 1988) and surface heat flux boundary conditions were used (Burgener and Reedy 1982). However, to study the localized heating ef-

fect in this work, the temperature profile along the direction perpendicular to the incident direction has to be considered, and thus a two-dimensional, transient heat conduction model is established. A volumetric heat-generation source with an exponentially decaying distribution in the propagation direction and with Gaussian distribution in the lateral direction is used to more accurately study the local temperature distribution. The absorption coefficient of silicon at 1064 nm is small, and this justifies the assumption of volumetric heat generation.

The schematic of the heat transfer through glass-silicon is shown in *Figure 2*. Pyrex™ glass is virtually transparent to the laser beam at the wavelength considered. Thus, the incident laser beam is primarily absorbed by silicon. Heat is conducted to the glass from the molten silicon, thereby softening the glass at the silicon-glass interface. Upon solidification, bonding is realized between the two layers.

The governing heat conduction equation in the glass layer is described as:

$$\rho c \frac{\partial T}{\partial t} = k \left[ \frac{\partial^2 T}{\partial z^2} + \frac{\partial^2 T}{\partial r^2} + \frac{1}{r} \frac{\partial T}{\partial r} \right] \quad (1)$$

The governing equation in silicon during laser irradiation is:

$$\rho c \frac{\partial T}{\partial t} = \frac{\partial}{\partial z} \left( k \frac{\partial T}{\partial z} \right) + \frac{\partial}{\partial r} \left( kr \frac{\partial T}{\partial r} \right) + Q_{ab}(z, r, t) \quad (2)$$

The energy absorption  $Q_{ab}$  in silicon is related to the incident laser intensity  $I_i$ , which is defined as:

$$I_i(r, t) = I_0 \exp\left(-\frac{r^2}{r_p^2}\right) \exp\left(-\frac{t^2}{t_p^2}\right) \quad (-\infty < t < +\infty) \quad (3)$$

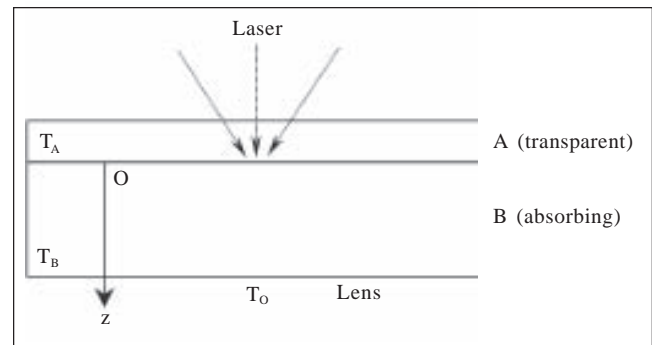


*Figure 2*  
 Schematic of Heat Transfer Through Glass (A) and Silicon (B)

where  $I_0$  is the maximum intensity of the laser pulse in the center at time  $t = 0$ . After reflection, the laser energy distribution in the silicon substrate is characterized as:

$$I = (1 - R)I_i \exp(-\alpha z) \quad (4)$$

The laser energy is attenuated in the medium and results in heat generation:

$$Q_{ab} = -\frac{\partial I}{\partial z} = (1 - R)\alpha I_i \exp(-\alpha z) \quad (5)$$

The laser pulse energy is related to  $I_0$ ,  $t_p$ , and  $r_p$  by:

$$J_0 = \int_{-\infty}^{\infty} \int_0^{\infty} I_i(r, t) 2\pi r dr dt = I_0 t_p r_p^2 \pi^{3/2} \quad (6)$$

The contact thermal resistance between silicon and glass is ignored because silicon and glass are in close contact by the application of force. Thus, the boundary condition at the interface is:

$$\left(k \frac{\partial T}{\partial z}\right)_g = \left(k \frac{\partial T}{\partial z}\right)_{si} \quad (7)$$

At the outer surface of the bi-layer system, the heat loss is assumed to be negligible because the heat loss is many orders of magnitude smaller compared to the heat generation (Chen and Tien 1994):

$$\frac{\partial T}{\partial z} = 0 \quad (8)$$

Because of the symmetry due to laser heating with a Gaussian-type intensity distribution, an adiabatic boundary condition is used at  $r = 0$ :

$$\frac{\partial T}{\partial r} = 0 \quad (9)$$

Initially, the temperature is uniformly distributed as:

$$T(z, r, 0) = 300 \text{ K} \quad (10)$$

Although the exact temperature of the bonding area during laser heating is unknown, it is reasonable to believe that it reaches or even exceeds the melting point of silicon. Thus, modeling phase-

change processes is necessary to predict the temperature in the bonding area. The phase-change modeling of silicon is achieved via an enthalpy method. Before phase change, the temperature change is related to enthalpy change by:  $dh = \rho c dT$ , while at phase change, additional enthalpy change includes the latent heat of fusion, which is  $1.8 \times 10^6$  J/kg for silicon (Hull 1999).

At room temperature, the penetration depth at 1064 nm is on the order of a few hundred micrometers, which ensures a volumetric heat generation over the whole thickness of the silicon substrate. However, as shown in *Figure 3*, at temperatures over 1000 K the absorption coefficient goes up to around  $2 \times 10^5 \text{ m}^{-1}$  (Jellison and Lowndes 1982) and the penetration depth reduces to a few micrometers. The increasing temperature results in stronger absorption in a much thinner layer, which in return greatly increases the local temperature. This effect is considered in our modeling and approximated by iteration. The absorption data at even higher temperatures are extracted from the available literature data extrapolated linearly for use in our modeling. Previous work (Hull 1999) has shown that the thermal conductivity of silicon as a function of temperature is approximately exponential until the melting point at 1687 K. The thermal conductivity data of silicon as a function of temperature used in simulation in this paper are shown in *Figure 4*. The thermal conduc-

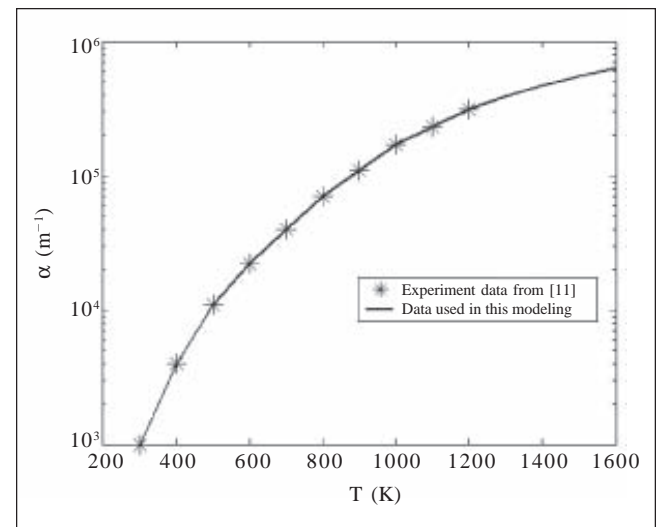


**Figure 3**  
Absorption Coefficient of Silicon at 1064 nm at Different Temperatures

tivity of silicon increases after melting due to the increased mobility of molecules and is assumed temperature-independent.

## Results and Discussion

The glass and silicon samples to be bonded were loaded onto the sample-holding device and pressure is applied to ensure a firm contact between the samples. A single laser pulse focused to a spot size of 800  $\mu\text{m}$  is used for bonding, and the corresponding pulse energy is measured using an energy meter (Nova Display, Ophir Optonics, Inc). The He-Ne laser used for probing is aligned with the heating spot using an alignment paper and focused to a spot of diameter 250  $\mu\text{m}$ . The silicon sample is melted due to absorption of the heating laser irradiation, and this results in a change in the intensity of the He-Ne laser beam reflected by the silicon sample. The variation in intensity of the reflected He-Ne beam is due to the change in reflectivity of silicon upon heating, as reflectivity depends both on the phase as well as on temperature. A signal captured by the oscilloscope during the bonding process is shown in *Figure 5*. From the figure, it is clear that the reflectivity of silicon increases until reaching a constant value. This increase in reflectivity is due to the phase change from solid to liquid as it dominates the change due to increase in temperature. In the liquid phase, silicon acts like a metal and the reflectivity is more than 90%. After about 40 ns, the liquid silicon starts to

solidify and the reflectivity decreases gradually depending on the cooling rate. Comparing the reflectivity values before and after melting, it is observed that the reflectivity values after bonding are slightly lower. This is due to the change in surface morphology at the interface due to melting and solidification of both silicon and glass.

The melting duration and the temperature of silicon are calculated numerically for heating by a single laser pulse (65 mJ energy and 800  $\mu\text{m}$  spot size). *Figure 6* shows the temperature history at different locations of the heating area. From the simulation, the melting time calculated for an area of diameter 280  $\mu\text{m}$  ( $0.35 R_0$ ) is found to be 35 ns. This compares well with the experimental value of 40 ns for a detecting area of diameter 250  $\mu\text{m}$ .

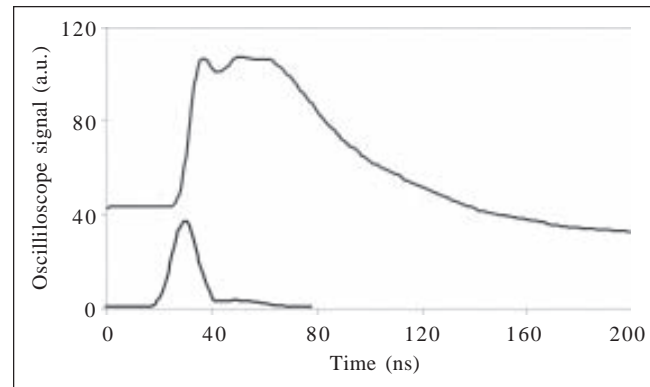


*Figure 5*  
 Change in Reflectivity of Silicon  
 During Laser Heating Measured In Situ

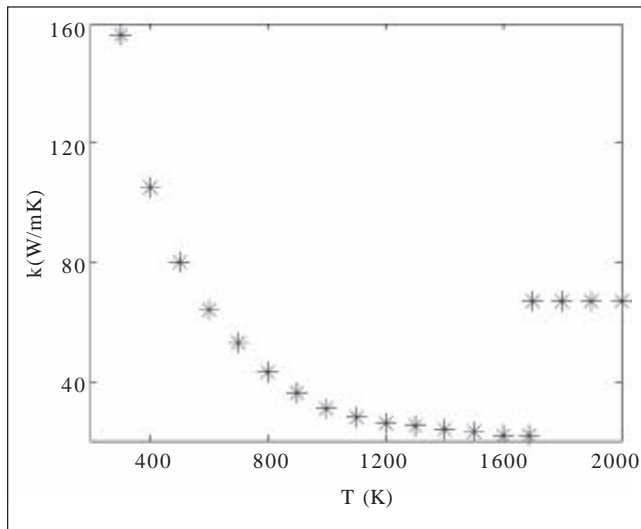


*Figure 4*  
 Thermal Conductivity of Silicon at Different Temperatures

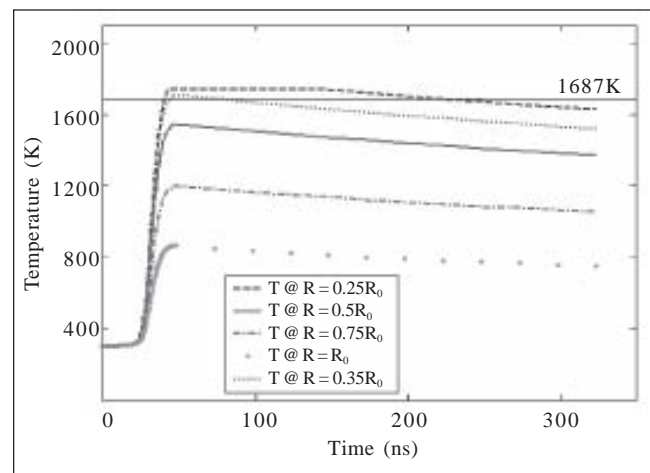


*Figure 6*  
 Silicon Surface Temperature History  
 at Different Locations After a Single Laser Pulse  
 (laser wavelength = 1064 nm, laser pulse = 12 ns,  
 laser energy = 65 mJ, laser beam diameter = 800  $\mu\text{m}$ )

The temperature distribution calculated for the entire heating area immediately after a single pulse is given in *Figure 7*. The center of the heating area of silicon attains a maximum temperature of 1867 K whereas at the periphery it is only about 700 K. This is due to the Gaussian energy distribution of the heating laser beam. From the figure, it is clear that about 40% of the heating area reaches a temperature above the melting point of silicon, which is about 1687 K. *Figure 8* shows the temperature distribution 300 ns after heating by a single pulse. At this time only the center of silicon remains molten whereas on the glass side almost a third of the heating area is at a temperature higher than the glass transition temperature, which is around 1100 K (Scholze 1991; Bansal 1986). This means that glass remains molten for a

longer duration than silicon due to the difference in thermal conductivity.

*Figure 9a* shows the schematic of a glass wafer on top of a silicon wafer. The laser heating was performed right on the edge of the glass sample to study the cross section of the bonded area. Here, half of the laser beam is within the glass wafer while another half is outside the glass wafer. The microscopic image, *Figure 9b*, shows the melting of silicon in the laser-processed area. *Figure 10a* is a microscopic image of the bonded interface, and this image clearly shows the joining of both silicon and glass at the bonding area. *Figure 10b* is an SEM micrograph showing the glass-silicon interface. Due to the pressure applied on both samples, the molten silicon is splashed and it can be seen on the sides of the glass

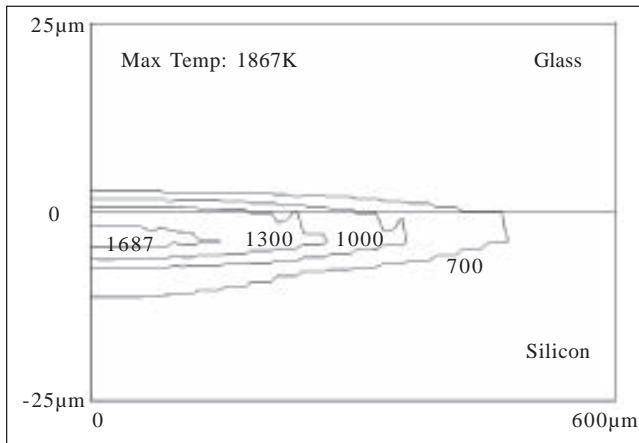


*Figure 7*

Temperature Contour of Both Glass and Silicon After a Single Laser Pulse (laser wavelength = 1064 nm, laser pulse = 12 ns, laser energy = 65 mJ, laser beam diameter = 800  $\mu\text{m}$ )

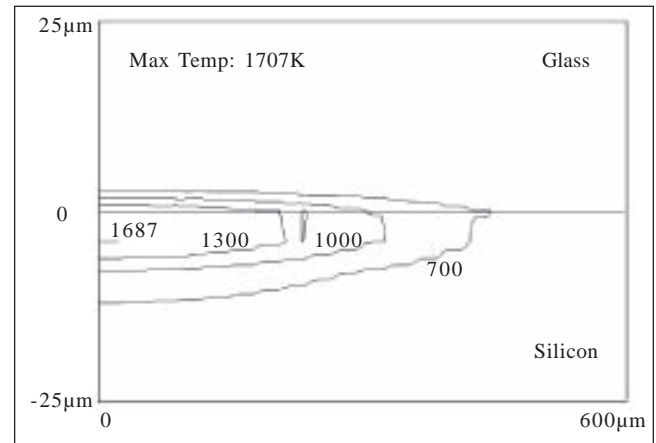


*Figure 8*

Temperature Contour 300 ns After a Single Laser Pulse (laser wavelength = 1064 nm, laser pulse = 12 ns, laser energy = 65 mJ, laser beam diameter = 800  $\mu\text{m}$ )

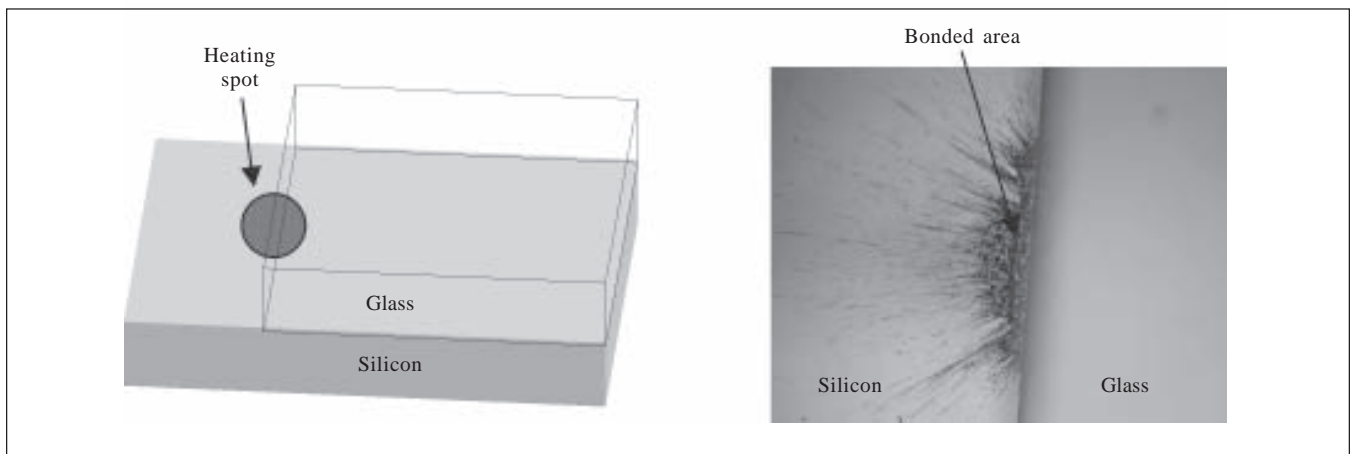


*Figure 9*

(a) Schematic showing bonded area at edge of glass sample, (b) corresponding optical microscopic image of bonded area

sample. The dependence of the bonding strength and bonding quality on the melting area and laser intensity are currently under investigation.

To study the bonding process in detail, the bonded glass-silicon sample was separated and observed under SEM. *Figure 11* shows a 400  $\mu\text{m}$  bonding area on both silicon and glass surfaces after irradiation with four different laser pulse energies. With an increase in pulse energy there is more melting, leading to an increase in the bonding area. An energy-dispersive spectroscopy (EDS) chemical analysis was also performed on the silicon sample, and the result is presented in *Figure 12*. The analysis shows the presence of Al and Na only in the bonded area of the silicon sample, thereby confirming the diffusion of Al and Na

components from glass into silicon during solidification. This is because of the longer melting duration of glass, which is still in the molten state when silicon starts to solidify. This shows that melting of both silicon and glass is essential for the bonding of glass and silicon.

## Conclusion

Glass and silicon wafers were joined together by using a pulsed Nd:YAG laser in the absence of an intermediate layer. This localized laser transmission joining technique provides a high temperature in a selected and localized region to achieve bonding while maintaining the whole wafer still at room temperature. A continuous wave He-Ne laser was used to provide online monitoring of the transient melt-

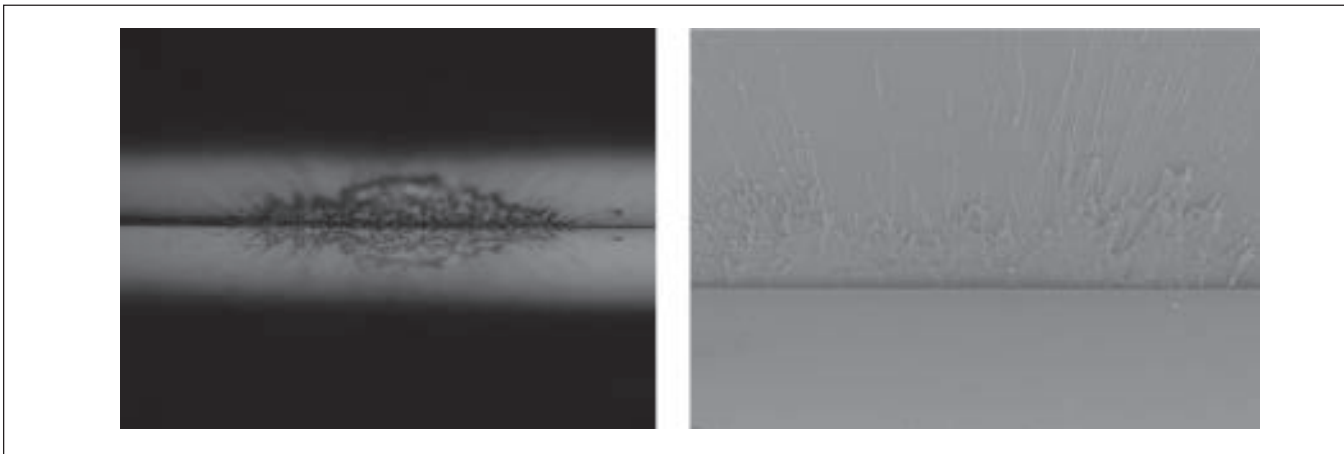


Figure 10

(a) Optical microscopic image of bonded area at glass-silicon interface, (b) SEM micrograph of glass-silicon interface

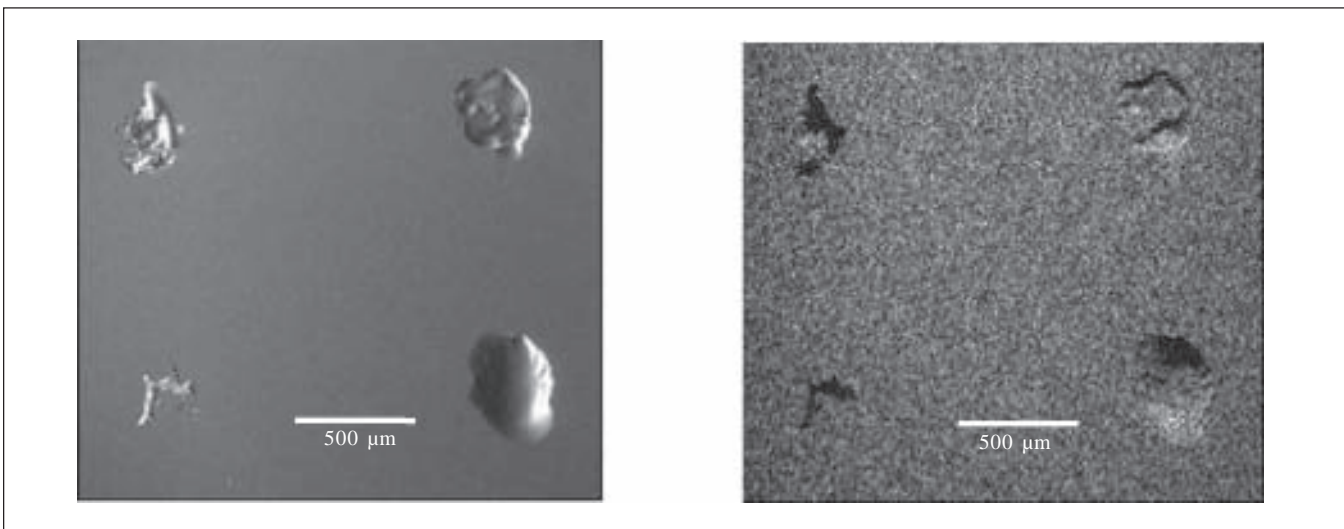


Figure 11

SEM Micrograph of Bonded Area After Separation: (a) on silicon side, (b) on glass side

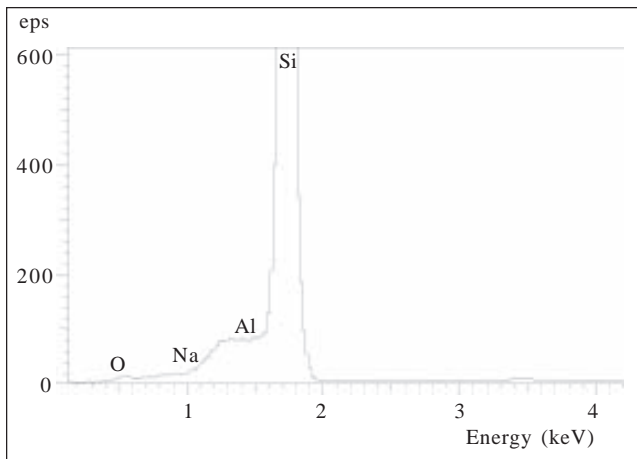


Figure 12  
Chemical Analysis of Bonded Area  
at Silicon Side of Interface

ing process of silicon upon pulsed laser heating. The online monitoring system is nonintrusive and gives reliable information about the melting and subsequent resolidification process. Estimates of the bonding time based on the finite element model compares well with the experimental results. Temperature profiles obtained during and after bonding suggest temperatures greater than the melting temperature and glass transition temperature of silicon and glass, respectively, at the bonding interface. The chemical analysis shows the presence of Al and Na in bonded areas of silicon. The diffusion of these components from glass is due to the longer melting duration of glass compared to silicon.

### Acknowledgment

This work was partially supported by U.S. National Science Foundation (DMI 0222014) and U.S. Dept. of Defense (N66001-03-1-8939). The SEM measurement was conducted in the Texas Materials Institute at the University of Texas at Austin.

### References

- Abraham, E. and Halley, J.M. (1987). "Some calculations of temperature profiles in thin films with laser heating." *Applied Physics A* (v42), pp279-285.
- Bansal, N.P. (1986). *Handbook of Glass Properties*. Orlando, FL: Academic Press.
- Bloisi, F. and Vicari, L. (1988). "Laser induced thermal profiles in thermally and optically thin films." *Applied Physics B* (v47), pp67-69.
- Bower, R.W. and Chin, F.Y.J. (1997). "Low temperature direct silicon wafer bonding using argon activation." *Japan Journal of Applied Physics, Part 2 (Letters)* (v36), pp. L527-L528.
- Bower, R.W.; Ismail, M.S.; and Roberts, B.E. (1993). "Low temperature Si<sub>3</sub>N<sub>4</sub> direct bonding." *Applied Physics Letters* (v62), pp3485-3487.

- Burgener, M.L. and Reedy, R.E. (1982). "Temperature distributions produced in a two layer structure by a scanning CW laser or electron beam." *Journal of Applied Physics* (v53), pp4357-4363.
- Chen, G. and Tien, C.L. (1994). "Thermally induced optical non-linearity during transient heating of thin films." *Journal of Heat Transfer* (v116), pp311-316.
- Hatano, M.; Moon, S.; Lee, M.; Suzuki, K.; and Grigoropoulos, C.P. (2000). "Excimer laser-induced temperature field in melting and resolidification of silicon thin films." *Journal of Applied Physics* (v87), pp36-43.
- Henmi, H.; Shoji, S.; Shoji, Y.; Yoshimi, K.; and Esashi, M. (1994). "Vacuum packaging for microsensors by glass-silicon anodic bonding." *Sensors and Actuators A* (v43), pp243-248.
- Hull, R. (1999). "Properties of crystalline silicon." INSPEC publication. London.
- Jellison, G.E. and Lowndes, D.H. (1982). "Optical absorption coefficient of silicon at 1.152  $\mu$  at elevated temperatures." *Applied Physics Letters* (v41), pp594-596.
- Luo, C. and Lin, L. (2002). "The application of nanosecond-pulsed laser welding technology in MEMS packaging with a shadow mask." *Sensors and Actuators A* (v97-98), pp398-404.
- Mescheder, U.M.; Alavi, M.; Hiltmann, K.; Lietzau, C.; Nachtigall, C.; and Sandmaier, H. (2002). "Local laser bonding for low temperature budget." *Sensors and Actuators A* (v97-98), pp422-427.
- Rogers, T. and Kowal, J. (1995). "Selection of glass, anodic bonding conditions and material compatibility for silicon-glass capacitive sensors." *Sensors and Actuators A* (v46-47), pp113-120.
- Scholze, H. (1991). *Glass: Nature, Structure, and Properties*. New York: Springer-Verlag.
- Wild, M.J.; Gillner, A.; and Poprawe, R. (2001). "Locally selective bonding of silicon and glass with laser." *Sensors and Actuators A* (v93), pp63-69.
- Xu, X.; Grigoropoulos, C.P.; and Russo, R.E. (1996). "Nanosecond-time-resolution thermal emission measurement during pulsed excimer-laser interaction with materials." *Applied Physics A* (v62), pp51-59.

### Authors' Biographies

Senthil Theppakuttai received the BS degree in mechanical engineering from the Regional Institute of Technology, Jamshedpur, India, in 1998 and MS in industrial and manufacturing systems engineering from Iowa State University in 2001. He is currently pursuing his PhD degree in the Mechanical Engineering Dept. at the University of Texas at Austin. His research focuses on micro/nanoscale laser materials processing and laser interaction with materials.

Dongbing Shao received the BE degree in engineering mechanics from Tsinghua University, Beijing, China, in 1998 and the MS degree in mechanical engineering from the University of Colorado at Boulder in 2002. Currently, he is a PhD candidate in the Mechanical Engineering Dept. at the University of Texas at Austin, working on micro/nanofabrication, nanophotonics, and electronics packaging.

Shaochen Chen received his PhD degree in mechanical engineering from the University of California-Berkeley in 1999. Currently, he is an assistant professor with in the Mechanical Engineering Dept. at the University of Texas at Austin. His research interests are in MEMS, laser materials processing, and thermal/fluid transport in micro/nanosystems. His research applications include biomedical engineering, microelectronics, and life science. Dr. Chen received the CAREER award from the U.S. National Science Foundation in 2001 and the Outstanding Young Manufacturing Engineer award from the Society of Manufacturing Engineers in 2002.